

1 **Title: Pubertal FGF21 deficit is central in the metabolic pathophysiology of an ovine**  
2 **model of polycystic ovary syndrome**

3

4 **Authors:** Katarzyna J. Siemienowicz<sup>a,b\*</sup>, Klaudia Furmanska<sup>b</sup>, Panagiotis Filis<sup>c</sup>, Chiara  
5 Talia<sup>c</sup>, Jennifer Thomas<sup>b</sup>, Paul A. Fowler<sup>c</sup>, Mick T. Rae<sup>b</sup>, W. Colin Duncan<sup>a</sup>

6

7 **Affiliations:** <sup>a</sup>MRC Centre for Reproductive Health, The University of Edinburgh, Edinburgh  
8 EH16 4TJ, UK; <sup>b</sup>School of Applied Sciences, Edinburgh Napier University, Edinburgh EH11  
9 4BN, UK; <sup>c</sup>Institute of Medical Sciences, School of Medicine, Medical Sciences & Nutrition,  
10 University of Aberdeen, Aberdeen AB25 2ZD, UK.

11

12 **\*Corresponding Author:**

13 Katarzyna J. Siemienowicz  
14 School of Applied Sciences,  
15 Edinburgh Napier University,  
16 Edinburgh EH11 4BN, UK

17 **Tel:** +44 (0)131 455 3458

18 **E-mail:** [k.siemienowicz@napier.ac.uk](mailto:k.siemienowicz@napier.ac.uk)

19

20 **Abstract**

21 Polycystic ovary syndrome (PCOS), affecting over 10% of women, is associated with insulin  
22 resistance, obesity, dyslipidaemia, fatty liver and adipose tissue dysfunction. Its  
23 pathogenesis is poorly understood and consequently treatment remains suboptimal.  
24 Prenatally androgenized (PA) sheep, a clinically realistic model of PCOS, recapitulate the  
25 metabolic problems associated with PCOS. Fibroblast Growth Factor 21 (FGF21) is a  
26 metabolic hormone regulating lipid homeostasis, insulin sensitivity, energy balance and  
27 adipose tissue function. We therefore investigated the role of FGF21 in the metabolic  
28 phenotype of PA sheep. In adolescence PA sheep had decreased hepatic expression and  
29 circulating concentrations of FGF21. Adolescent PA sheep show decreased FGF21  
30 signalling in subcutaneous adipose tissue, increased hepatic triglyceride content, trend  
31 towards reduced fatty acid oxidation capacity and increased hepatic expression of  
32 inflammatory markers. These data parallel studies on FGF21 deficiency, suggesting that  
33 FGF21 therapy during adolescence may represent a treatment strategy to mitigate  
34 metabolic problems associated with PCOS.

35

36 **Keywords:** polycystic ovary syndrome, Fibroblast Growth Factor 21 (FGF21), metabolism,  
37 prenatal programming, androgens

38

39 **1. Introduction**

40 Polycystic ovary syndrome (PCOS), affecting over 10% of women, is associated with  
41 increased risk of hyperinsulinemia, insulin resistance, obesity, dyslipidemia and non-  
42 alcoholic fatty liver disease (NAFLD) (Fauser et al., 2012; Moran et al., 2015; Teede et al.,  
43 2010). In addition, PCOS women have enlarged subcutaneous adipose tissue (SAT)  
44 (Echiburú et al., 2018; Manneras-Holm et al., 2010), lower levels of circulating adiponectin  
45 (Escobar-Morreale et al., 2006; Maliqueo et al., 2012) and increased abdominal adiposity  
46 independent of BMI. Taken together, these indicate adipose tissue dysfunction, which  
47 further correlates with an adverse metabolic profile (Puder et al., 2005; Yildirim et al., 2003).  
48 Metabolic comorbidities associated with the syndrome worsen with age, negatively  
49 impacting health and wellbeing of women, and health service resources (Jason, 2011;  
50 Teede et al., 2010). The pathogenesis of PCOS remains poorly understood, and, in the  
51 absence of mechanistic understanding, treatment remains suboptimal.

52  
53 Hepatic-derived Fibroblast Growth Factor 21 (FGF21) is a metabolic hormone, regulating  
54 glucose and lipid homeostasis, insulin sensitivity, energy balance and adipose tissue  
55 function (Fisher and Maratos-Flier, 2016; Lewis et al., 2019). Animals overexpressing  
56 FGF21 in the liver have improved insulin sensitivity, reduced triglyceride (TG)  
57 concentrations and are resistant to diet-induced obesity (Jimenez et al., 2018;  
58 Kharitonov et al., 2005). FGF21 knockout (FGF21-KO) mice have hyperinsulinemia with  
59 increased proliferation of pancreatic beta cells (So et al., 2015), increased hepatic fat  
60 content (Badman et al., 2009; Tanaka et al., 2015), and display delayed weight gain with  
61 mild obesity after 24 weeks on standard diet (Badman et al., 2009). FGF21 regulates the  
62 activity of PPARG (Dutchak et al., 2012), the master regulator of adipogenesis. FGF21  
63 deficient mice have defects in PPARG signalling and decreased body fat (Dutchak et al.,

64 2012). In rodents and monkeys, FGF21 treatment improved insulin sensitivity, reduced  
65 serum lipids and attenuated hepatic fat accumulation and inflammation (Kharitononkov et  
66 al., 2007; Xu et al., 2009a; 2009b; Zhu et al., 2014). In human clinical trials, though  
67 treatment with FGF21 showed only modest improvement in glycaemic control, it  
68 consistently improved plasma lipid profiles and decreased hepatic fat content and serum  
69 markers of liver fibrosis in patients with NASH (Lewis et al., 2019; Sanyal et al., 2019).

70

71 Prenatal androgen overexposure is associated with a PCOS-phenotype in adult life (Risal  
72 et al., 2019). Daughters of women with PCOS have increased cord blood testosterone  
73 (Daan et al., 2017) and longer anogenital distance (Barrett et al., 2018) indicating increased  
74 *in utero* androgen exposure. Prenatally androgenized sheep is a clinically realistic model of  
75 PCOS (Padmanabhan and Veiga-Lopez, 2013), manifesting ovarian, hormonal and  
76 metabolic phenotypes reminiscent of PCOS (Connolly et al., 2014; Hogg et al., 2011, 2012;  
77 Rae et al., 2013; Ramaswamy et al., 2016), used to provide insights into the molecular  
78 pathophysiology of PCOS and to examine therapeutic paradigms (Connolly et al., 2014).

79 We have previously shown, using ovine models of PCOS, that adolescent prenatally  
80 androgenized (PA) sheep had hyperinsulinaemia, increased pancreatic beta cell content,  
81 fatty liver, diminished adipogenesis in SAT accompanied by decreased levels of leptin and  
82 adiponectin, and increased circulating free fatty acids (FFAs), independent of obesity and  
83 adiposity (Hogg et al., 2011; Rae et al., 2013; Siemienowicz et al., 2021). Adult PA sheep  
84 had decreased postprandial thermogenesis, increased body weight and insulin resistance  
85 (Siemienowicz et al., 2020). Decreased adipocyte differentiation during adolescence in PA  
86 sheep resulted in hypertrophy and inflammation of adult SAT, paralleled by elevated FFAs  
87 concentrations of and increased expression of genes linked to fat accumulation in visceral  
88 adipose tissue (VAT) (Siemienowicz et al., 2021). In view of the clinically relevant metabolic

89 perturbations present in adolescent and adult prenatally androgenized sheep, and intriguing  
90 parallels to models of FGF21 manipulation, we hypothesised that dysregulated FGF21  
91 action had a role in the metabolic phenotype in PA sheep. Herein, supporting our  
92 hypothesis, we report FGF21 expression, as well adipose tissue and hepatic changes  
93 related to FGF21, during the development of metabolic disturbances seen in an ovine  
94 model of PCOS.

95

96 **2. Materials and Methods**

97 **2.1 Ethics statement**

98 All studies were approved by the UK Home Office and conducted under approved Project  
99 Licence PPL60/4401. The Animal Research Ethics Committee of The University of  
100 Edinburgh approved this study. The study was carried out in accordance with the relevant  
101 guidelines.

102 **2.2 Animals**

103 Animal husbandry, experimental protocols and tissue collection were performed as  
104 previously described (Hogg et al., 2011; 2012; Rae et al., 2013; Ramaswamy et al., 2016).  
105 Scottish Greyface ewes were housed in groups in spacious enclosures and fed hay *ad*  
106 *libitum*. Ewes with a healthy body condition score (2.75-3) were synchronised with  
107 Chronogest (flugestone) sponges (Intervet Ltd, UK) and Estrumate (cloprostenol) injection  
108 (Schering Plough Animal Health, UK) then mated with Texel rams. Pregnancy was  
109 suggested by lack of estrous, then confirmed by ultrasound scanning.

110 In the maternal injection cohort (MI) pregnant ewes were randomised to twice weekly IM  
111 100mg testosterone propionate (TP) in 1ml vegetable oil from day (D)62 to D102 of D147  
112 pregnancy or 1ml vegetable oil (control (C)). In pregnancies where fetal tissue was  
113 collected (D112: C=9; PA=4), ewes were sacrificed on D112 of gestation via barbiturate  
114 overdose. The gravid uterus was immediately removed, fetal sex and weight recorded, and  
115 tissue of interest snap frozen and stored at -80C. In pregnancies carried to term, lambs  
116 were weaned at 3 months and fed hay and grass *ad libitum* until sacrifice at 11 weeks  
117 [juvenile (C=8; PA=8)]; 11 months, [adolescent (C=5; PA=9)] or 30 months [adult (C=11;  
118 PA=4)].

119 To further examine the effects of androgen we developed a further cohort where the fetuses  
120 were directly injected. In the fetal injection cohort (FI), on day 62 and day 82 of gestation,

121 mothers were randomised and anaesthetised by initial sedation with 10 mg Xylazine (i.m.  
122 Rompun; Bayer PLC Animal Health Division, UK), followed by 2mg/kg Ketamine (i.v,  
123 Ketaset; Fort Dodge Animal Health, UK). All subsequent procedures were conducted under  
124 surgical aseptic conditions. Fetuses were injected via ultrasound guidance into the fetal  
125 flank with 20G Quinke spinal needle (BD Biosciences, UK) with following according to the  
126 treatment group: control (C; n=12), 0.2ml vehicle (vegetable oil); testosterone propionate  
127 (PA; n=15), 20mg TP in 0.2ml vehicle; diethylsilbesterol (DES; n=8), 4mg DES in 0.2ml  
128 vehicle. In this study we maintained the males until adolescence and could investigate a  
129 cohort of males, controls (C; n=14) and testosterone propionate (PA; n=14). Justification of  
130 the rationale, timing and treatment doses have been published previously (Siemienowicz et  
131 al., 2019). Immediately after surgical procedure completion all pregnant ewes were given  
132 prophylactic antibiotics (Streptacare, Animalcare Ltd., UK, 1 ml/25 kg) and were then  
133 monitored during recovery; no adverse effects of these procedures were observed. Lambs  
134 were weaned at 3 months and fed hay and grass *ad libitum* and sacrificed in adolescence  
135 (11 months of age for females and 6 months of age for males).

### 136 **2.3 Tissue collection**

137 Fasting blood samples were collected just prior to sacrifice and plasma was separated and  
138 stored at -20°C. For adult ewes an additional blood sample was collected at 22 months of  
139 age. Liver sampling occurred from the same lobe (right posterior), in approximately the  
140 same area. Liver samples from MI cohort were collected from fetuses at D112 of gestation,  
141 and from females at 11 weeks, 11 months and 30 months of age. From FI cohort livers  
142 were collected from females at 11 months of age and from males at 6 months of age.  
143 Subcutaneous adipose tissue (SAT) was collected from the groin region and visceral  
144 adipose tissue (VAT) from omentum. Adipose tissue was collected from females from MI

145 cohort at 11 months and 30 months of age. Tissues were immediately snap frozen, then  
146 stored at  $-80^{\circ}\text{C}$  until further processing.

#### 147 **2.4 Plasma analyte determination**

148 Concentrations of fasting plasma free fatty acids (FFAs) and triglycerides (TGs) were  
149 obtained using commercial assay kits (Alpha Laboratories Ltd., UK) as per manufacturer's  
150 instruction, using a Cobas Mira automated analyser (Roche Diagnostics Ltd, UK). Assay  
151 intra and inter-assay CV's were  $< 4\%$  and  $< 5\%$  respectively. Plasma FGF21 was  
152 measured using human FGF21 ELISA kit (ab125966; Abcam Cambridge, UK) as per  
153 manufacturer's instructions. All samples were assayed in duplicate. The assay sensitivity  
154 was  $0.03\text{ ng/ml}$ ; intra and inter-assay CVs were  $4.7\%$  and  $7.2\%$  respectively.

#### 155 **2.5 Hepatic triglyceride determination**

156 Hepatic triglyceride content was measured using Triglyceride Determination Kit (TR0100,  
157 Sigma-Aldrich, Merck, UK). Briefly, liver tissue was cut on dry ice, weighed and  
158 homogenized in PBS. Next, samples were centrifuged at room temperature for 30 seconds  
159 at  $16000g$ , lipid phase was removed, and all samples were assayed in duplicate, following  
160 manufacturer's instructions.

#### 161 **2.6 Quantitative (q)RT-PCR**

162 RNA was extracted from adipose tissue with TRI Reagent combined with the RNeasy Mini  
163 Kit (Qiagen Ltd.), and from liver using RNeasy Mini Kit following manufacturer's  
164 instructions. On-column DNase digestion was performed using RNase-Free DNase set  
165 (Qiagen Ltd.), and RNA concentration and purity assessed using a NanoDrop One  
166 spectrometer (ThermoFisher Scientific, UK). Complimentary DNA was synthesised using  
167 TaqMan Reverse Transcription Kit (Applied Biosystems, UK) as described previously (Hogg  
168 et al., 2012). To select the most stable housekeeping genes the geNorm Reference Gene



169 Selection Kit (Primerdesign Ltd., UK) was used, identifying the suitability of the geometric  
170 mean of *ACTB* and *MDH1* for liver and SAT, and *RPS26* and *18S* for VAT.  
171 Primers (Supplementary Table 1) were designed and synthesised as described previously  
172 (Siemienowicz et al., 2020). Quantitative RT-PCR was performed on 384-well plate format  
173 (Applied Biosystems) with all samples assayed in duplicate and housekeeping control  
174 genes included in each run, as well as template, RNA and RT-negative controls, using the  
175 ABI 7900HT Fast Real Time PCR system (Applied Biosystems) as described previously  
176 (Hogg et al., 2012). The transcript abundance of target gene relative to the housekeeping  
177 genes was quantified using the  $\Delta\Delta C_t$  method (Livak and Schmittgen, 2001).

## 178 **2.7 RNA sequencing transcriptomic analyses**

179 RNA sequencing experiment was previously described in detail (Siemienowicz et al., 2019).  
180 Briefly, libraries were prepared with the Illumina TruSeq Stranded mRNA kit. Sequencing  
181 was performed on the NextSeq 500 High Output v2 kit (75 cycles) on the Illumina NextSeq  
182 500 platform. To assess quality of sequencing data, reads were analysed with FastQC. To  
183 remove any lower quality and adapter sequences, TrimGalore! was used. To remove the  
184 ERCC reads, all reads were aligned to the ERCC reference genome using HISAT2. These  
185 alignments were processed using SAMtools, reads were counted using featureCounts and  
186 analysed using the R package erccdashboard. Reads were aligned to reference genome  
187 using HISAT2. SAMtools was used to process the alignments and reads were counted at  
188 gene locations using featureCounts. Pairwise gene comparisons were carried out using  
189 edgeR on all genes with CPM (count per million) value of more than one in six, the  
190 remainder removed as low count genes.

## 191 **2.8 Statistical analysis**

192 All data sets were normality tested prior to further analysis (Shapiro-Wilk test), and  
193 logarithmically transformed if necessary. For comparing means of two treatment groups

194 with equal variances, unpaired, two-tailed Student's t test was used accepting  $P < 0.05$  as  
195 significant. Correlation was assessed by calculation of Pearson product-moment co-  
196 efficient. Statistical analysis was performed using GraphPad Prism 8.0 software (GraphPad  
197 Prism Software, San Diego, CA, USA). Asterisks were used to indicate level of significance  
198 based on the following criteria: \* $P < 0.05$ , \*\* $P < 0.01$ .  
199

## 200 **3. Results**

### 201 **3.1 FGF21 is reduced during adolescence in PA sheep**

202 To determine whether the metabolic disturbances previously reported (Hogg et al., 2011;  
203 Rae et al., 2013; Siemienowicz et al., 2020; 2021) in PA sheep from MI cohort were  
204 associated with altered FGF21 production, hepatic expression, and circulating  
205 concentrations, of FGF21 were assessed. There was no difference in hepatic FGF21  
206 expression in fetal (Fig. 1A), juvenile (pre-pubertal) (Fig. 1B) or in adult life (Fig. 1D).  
207 Hepatic *FGF21* was reduced in adolescent PA sheep at 11 months of age by 79% as  
208 compared with controls (Fig. 1C;  $P < 0.01$ ). The changes in the hepatic *FGF21* expression  
209 were mirrored by circulating FGF21, with reduced levels in adolescence (C;  $0.9 \pm 0.29$   
210 ng/ml vs PA;  $0.57 \pm 0.25$  ng/ml) and in the early adulthood at 22 months of age (C;  $0.76 \pm$   
211  $0.26$  ng/ml vs PA;  $0.45 \pm 0.13$  ng/ml), that normalised in adulthood at 30 months of age (C;  
212  $0.87 \pm 0.39$  ng/ml vs PA;  $0.63 \pm 0.45$  ng/ml) (Fig. 1E;  $P < 0.05$ ). Since FGF21 induces  
213 *PPARGC1A* (Potthoff et al., 2009; Ye et al., 2014) we examined hepatic *PPARGC1A*  
214 expression and observed that adolescent PA sheep showed a strong trend for decreased  
215 *PPARGC1A* (Fig. 1F;  $P = 0.054$ ). There was no difference in the expression of *PPARGC1A*  
216 between controls and PA sheep in adulthood (Fig. 1G). In addition, we noted a significant  
217 correlation between hepatic *FGF21* and *PPARGC1A* expression in the adolescent liver  
218 (Fig. 1H;  $P < 0.001$ ). There is a window in adolescence in PA sheep where there is reduced  
219 FGF21.

220

### 221 **3.2 There is decreased FGF21 signalling in the SAT of adolescent PA sheep**

222 Adipose tissue is the primary target of FGF21 action (Véniant et al., 2012) where it  
223 upregulates the activity of PPARG (Dutchak et al., 2012), the master regulator of  
224 adipogenesis, and results in increased adiponectin expression (Lin et al., 2013). As we

225 have previously shown that both *PPARG* and *ADIPOQ* were significantly downregulated in  
226 SAT of adolescent PA sheep (Siemienowicz et al., 2021) we examined the expression of  
227 *FGFR1* and its *KLB* co-receptor, which regulate *FGF21* action, in adipose tissue.  
228 In adolescence, in SAT there was a reduction of *KLB* with similar levels of *FGFR1* (Fig. 2A;  
229  $P < 0.05$ ) while there was no difference in the expression of *KLB* and *FGFR1* in VAT (Fig.  
230 2B). Conversely, in adulthood there was no differences in *KLB* and *FGFR1* in SAT (Fig. 2C)  
231 however, both *KLB* and *FGFR1* were increased in the VAT of PA sheep when compared to  
232 controls (Fig. 2D;  $P < 0.05$ ). In addition, apart from *PPARG* in adult VAT, there was a  
233 positive correlation between *KLB* and *PPARG* expression (Fig. 2E;  $P < 0.01-0.0001$ ) and  
234 *ADIPOQ* expression (Fig. 2E;  $P < 0.05-0.0001$ ) in both VAT and SAT, in adolescence (11M)  
235 and adulthood (30M) (Fig. 2E).

236

### 237 **3.3 Reduction in *FGF21* and *PPARGC1A* expression is androgen and sex specific**

238 Maternal androgen injection during gestation increases fetal androgen concentrations as  
239 well as estrogen concentrations as a result of placental aromatisation (Rae et al., 2013). To  
240 further investigate the direct role of prenatal androgens in the 'programming' of these  
241 metabolic alterations, we assessed hepatic *FGF21* expression in animals directly injected  
242 with steroid hormones during fetal life. Adolescent female sheep directly injected with  
243 testosterone in fetal life have a closely comparable metabolic profile to sheep exposed to  
244 increased androgens *in utero* through maternal injections (Hogg et al., 2011; Ramaswamy  
245 et al., 2016; Siemienowicz et al., 2021). Expression of *FGF21* was reduced in adolescent  
246 prenatally androgenised females when assessed through RNAseq (Fig. 3A;  $P < 0.05$ ) and  
247 qRT-PCR (Fig. 3B;  $P < 0.05$ ), and there was a positive correlation between RNAseq and  
248 qRT-PCR results (Fig. 5C;  $P < 0.0001$ ), extending confidence in parallels between both  
249 models and technical assays. Comparable to maternal injection model, adolescent females

250 directly treated with testosterone *in utero* had decreased hepatic expression of *PPARGC1A*  
251 (Fig. 3D;  $P < 0.01$ ). Hepatic expression of *FGF21* (Fig. 3E) and *PPARGC1A* (Fig. 3F) was no  
252 different in adolescent females exposed to prenatal estrogens *in utero*, suggesting direct  
253 androgenic programming. There was and no difference in *FGF21* (Fig. 3. G) and  
254 *PPARGC1A* (Fig. 3H) adolescent males directly exposed to elevated levels of androgens in  
255 fetal life, suggesting sex-specificity of this prenatal in utero androgen excess model.

256

### 257 **3.4 Adolescent PA sheep have decreased hepatic lipid oxidation and increased** 258 **hepatic lipid content and inflammation**

259 As *FGF21* can improve lipid profiles and reduce hepatic fat content we investigated the liver  
260 in detail in the PA female animals during adolescence using the FI model. In these sheep  
261 there was a trend for increased circulating free fatty acids (Fig. 4A;  $P = 0.07$ ). We assessed  
262 fatty acid oxidation in the liver in different cellular compartments. In the mitochondrial  
263 compartment prenatally androgenized sheep had decreased expression of hepatic *CPT1B*  
264 (Fig. 4B;  $P < 0.05$ ) with a trend towards reduced expression of *SLC25A20* (Fig. 4B;  $P = 0.07$ )  
265 and *CPT2* (Fig 4B;  $P = 0.06$ ) that are rate-limiting factors, with regards to getting fatty acids  
266 into the mitochondria for beta oxidation (Fig. 4B). There was no difference in the expression  
267 of genes associated with mitochondrial beta oxidation (Fig.4C).

268 With regards to beta oxidation in the peroxisomes, there was decreased expression of  
269 *ABCD3* (Fig. 4D;  $P < 0.05$ ) and *ACAA1* (Fig. 4D;  $P < 0.05$ ), genes involved in the initial  
270 peroxisomal beta oxidation of larger fatty acids. The endoplasmic reticulum is responsible  
271 for omega oxidation and prenatally androgenized sheep had decreased expression of  
272 *CYP4F11* (Fig. 4E;  $P < 0.05$ ) and a trend towards decreased *CYP4F3* (Fig.4E;  $P = 0.058$ ) and  
273 *CYP4A11* (Fig. 4E;  $P = 0.06$ ), which are key genes involved in omega oxidation. Overall  
274 there was a consistent trend for reduced fatty acid oxidation and this is associated with

275 increased hepatic triglyceride content (Fig. 4F). There was a positive correlation between  
276 hepatic *PPARGC1A* expression and genes involved in lipid oxidation (Table 1;  $P < 0.05$ -  
277 0.0001).

278 Dysregulated immune response play a central role in the development and progression of  
279 NAFLD (Gao and Tsukamoto, 2016; Oates et al., 2019). Adolescent PA sheep had  
280 increased expression of molecular markers of classically activated, pro-inflammatory (M1)  
281 macrophages, *CD68*, *ADGRE1*, *TLR2* and *TLR4* (Fig. 5A;  $P < 0.05$ -0.01), a trend for  
282 increased *CD86* (Fig. 5A;  $P = 0.054$ ) and *IL1R* (Fig. 5A;  $P = 0.07$ ). In addition, there was  
283 increased expression of proinflammatory cytokines *IL1B* and *IL18* (Fig. 5B;  $P < 0.05$ ), and  
284 chemokines *CXCL9*, *CXCL10* and *CCL5* (Fig. 5C;  $P < 0.05$ ). Overall the PA female  
285 adolescent ewes with reduced FGF21 show reduced fatty acid usage in the liver as well as  
286 increased liver fat and increased liver inflammation.

287

#### 288 4. Discussion

289 Prenatally androgenized sheep had decreased hepatic expression and circulating  
290 concentrations of FGF21 in adolescence (11M) and during the transition from adolescence  
291 to adulthood (22M). FGF21 is a primarily hepatic hormone, which regulates glucose  
292 metabolism, insulin sensitivity, lipid homeostasis and energy balance (Lewis et al., 2019).  
293 FGF21 knockout (FGF21-KO) mice are hyperinsulinemic. These animals exhibit increased  
294 pancreatic beta cell proliferation (So et al., 2015), increased hepatic fat content (Badman et  
295 al., 2009; Tanaka et al., 2015), decreased expression of hepatic PGC1 $\alpha$  (encoded by  
296 *PPARGC1A*) involved in fatty acid  $\beta$ -oxidation (Badman et al., 2009), increased hepatic  
297 macrophage infiltration and pro-inflammatory cytokines (Liu et al., 2016). As a result, they  
298 display delayed weight gain with mild obesity after 24 weeks on standard diet (Badman et  
299 al., 2009). Taken together with our data showing decreased expression of FGF21 and  
300 altered associated receptor and metabolic systems in prenatally androgenized sheep, we  
301 conclude that lowered FGF21 in adolescence contributes to the perturbed metabolic  
302 phenotype in PCOS.

303

304 Our adolescent sheep, from both models employed in the current study (indirect and direct  
305 exposure to increased androgens *in utero*), have hyperinsulinemia and increased  
306 pancreatic beta cell content (Rae et al., 2013; Ramaswamy et al., 2016), fatty liver (Hogg et  
307 al., 2011), and decreased energy expenditure with increased body weight in adulthood  
308 (Siemienowicz et al., 2020). We have now confirmed increased hepatic triglyceride content  
309 in adolescent sheep directly treated with androgens *in utero*, and further demonstrated  
310 decreased hepatic *PPARGC1A* expression, reduced fatty acid oxidation capacity and  
311 increased hepatic expression of inflammatory markers in adolescent PA sheep. This series  
312 of parallels between models of FGF21 manipulation, and prenatal androgen exposure,

313 direct us to conclude that FGF21 reduction during adolescence is a critical component  
314 underpinning the metabolic profile which develops in adulthood in such PA models.  
315  
316 Adipose tissue is the primary target of FGF21 action (Véniant et al., 2012), in which it  
317 preferentially binds to FGFR1 linked to KLB co-receptor (Yang et al., 2012), a key  
318 component of FGF21 signalling (Ding et al., 2012). Consequently, beneficial effects of  
319 FGF21 treatment as regards decreasing fat mass, restoring insulin sensitivity and reducing  
320 blood lipids are compromised in mice with adipocyte-selective ablation of FGFR1 (Adams et  
321 al., 2012b) or KLB (Adams et al., 2012a). FGF21 functions in a feed-forward loop in  
322 adipose tissue, regulating PPARG activity, considered to be the 'master regulator' of  
323 adipogenesis (Dutchak et al., 2012). Evidentially, FGF21 deficient mice have defects in  
324 PPARG signalling and decreased body fat (Dutchak et al., 2012), with selective SAT  
325 volume reduction, but no changes in VAT (H. Li et al., 2018).  
326  
327 FGF21 treatment promotes SAT expansion, through adipocyte hyperplasia, and reverses  
328 insulin resistance in FGF21-KO mice (H. Li et al., 2018). Hepatic overexpression of FGF21  
329 in obese mice reverses adipocyte hypertrophy and inflammation (Jimenez et al., 2018).  
330 SAT is considered a healthy fat depot and is thought to be protective while increased VAT  
331 volume correlated with pathologic inflammation and insulin resistance (Booth et al., 2014).  
332 In humans, serum FGF21 concentration and *KLB* expression in SAT positively correlate  
333 with the SAT volume and maintenance of insulin sensitivity (H. Li et al., 2018). Collectively  
334 this indicates that FGF21 acts as selective regulator of the SAT storage capacity, and SAT  
335 is an important component as regards positive effects of FGF21 on insulin sensitivity.  
336 FGF21-KO mice have decreased expression of *KLB*, *PPARG*, *CEBPA*, *INSR*, *IRS1*, and  
337 *SLC2A4* in adipose tissue, particularly in SAT (Badman et al., 2009; Dutchak et al., 2012;



338 H. Li et al., 2018) and when fed high-fat diet, they have elevated circulating FFA, increased  
339 hepatic fat accumulation and enlarged adipocytes (Dutchak et al., 2012). These metabolic  
340 phenotypes parallel our ovine model of PCOS, with adolescent PA sheep having decreased  
341 FGF21 concentration, decreased expression of *KLB*, adipogenesis markers (*PPARG*,  
342 *CEBPA* and *CEBPB*) and reduced insulin signalling potential in SAT, but not VAT, while  
343 adult PA sheep present with obesity, elevated circulating FA and adipocyte hypertrophy and  
344 reduced adipogenesis in SAT, but not VAT (Siemienowicz et al., 2021). This data provides  
345 a compelling case for targeting SAT expansion in adolescence through FGF21 treatment,  
346 representing a novel therapeutic strategy to combat metabolic problems associated with  
347 PCOS.

348

349 Adiponectin, an insulin sensitizing, anti-inflammatory and hepatoprotective factor  
350 synthesized by adipocytes, is a critical downstream effector of FGF21 (Lin et al., 2013).  
351 FGF21 induces adiponectin gene expression and secretion from adipocytes through a  
352 *PPARG* dependent mechanism (Lin et al., 2013). The effects of FGF21 treatment on  
353 regulating insulin sensitivity, alleviation of dyslipidaemia, NAFLD and NASH are dependent  
354 on the presence of adiponectin (Bao et al., 2018; Holland et al., 2013; Lin et al., 2013). We  
355 recently demonstrated that adolescent PA sheep have decreased adiponectin levels  
356 paralleled by decreased *ADIPOQ* expression in SAT (Siemienowicz et al., 2021), which is  
357 mirrored in adolescent and adult women with PCOS (Cankaya et al., 2014; Escobar-  
358 Morreale et al., 2006; Maliqueo et al., 2012). FGF21-KO mice have low levels of circulating  
359 adiponectin, while treatment with recombinant FGF21 increases serum adiponectin in those  
360 animals (Lin et al., 2013). This link between FGF21 and adiponectin is further emphasized  
361 by clinical trials, where administration of an FGF21 analogue to patients with NAFLD or  
362 type 2 diabetes and non-human primates resulted in increased circulating adiponectin

363 levels in dose-dependent manner (Gaich et al., 2013; Sanyal et al., 2019; Talukdar et al.,  
364 2016). Furthermore, in age 6-18 humans FGF21 concentration is positively correlated with  
365 adiponectin concentration, and an overall healthier metabolic profile, whereas children with  
366 diminished FGF21 had highest proportion of insulin resistance and metabolic syndrome (G.  
367 Li et al., 2017).

368

369 In the pediatric population, FGF21 deficiency is considered to play a role in the  
370 pathogenesis of insulin resistance, components of metabolic syndrome, fatty liver and low  
371 levels of adiponectin, independent of BMI (Alisi et al., 2013; G. Li et al., 2017). Interestingly,  
372 males have lower levels of FGF21 than females during puberty (Bisgaard et al., 2014; G. Li  
373 et al., 2017) and adulthood (Hanssen et al., 2015). Therefore, it is possible that sex  
374 hormones might have a role in regulation of FGF21 expression. There are no studies  
375 investigating FGF21 levels in adolescent girls with PCOS. Adult women with PCOS were  
376 reported to have comparable FGF21 levels with BMI-matched controls (Gorar et al., 2010;  
377 Sahin et al., 2014), again, matching our observations, in that there was no difference in  
378 FGF21 levels between adult controls and PCOS-like sheep.

379

380 The metabolic consequences of PCOS can be extremely serious. NAFLD describes a  
381 spectrum of liver pathologies, from simple hepatic steatosis, characterized by more than 5%  
382 fat infiltration to non-alcoholic steatohepatitis (NASH), a combination of hepatocellular  
383 injury, inflammation, and an increased risk of liver fibrosis (Fazel et al., 2016). PCOS  
384 sufferers are at increased risk of developing NAFLD and are likely to have more severe  
385 forms of NAFLD (Sarkar et al., 2020). The estimated prevalence of NAFLD in women with  
386 PCOS varies between 34 to 70%, compared to 25 to 30% in the general population  
387 (Paschou et al., 2020); during adolescence, there is more than double the incidence of

388 NAFLD as when compared with non-PCOS girls (Ayonrinde et al., 2016). FGF21 deficiency  
389 promotes the development of steatosis, hepatic inflammation, hepatocyte damage, and  
390 fibrosis, whereas FGF21 treatment ameliorates NASH by attenuating these processes  
391 (Zarei et al., 2020). Likewise, genetic polymorphism that reduce PGC1 $\alpha$  expression  
392 correlates with the development of NAFLD in children and adults (Lin et al., 2013; Yoneda et  
393 al. 2008), while in NAFLD patients expression of PGC1 $\alpha$  is decreased (Westerbacka et al.,  
394 2007). In the paediatric population hepatic FGF21 is inversely correlated with non-alcoholic  
395 fatty liver progression (Alisi et al., 2013). In adult population however the opposite is true,  
396 with higher levels of FGF21 in patients with NAFLD and NASH, positively correlating with  
397 the disease progression (Barb et al., 2019; Dushay et al., 2010), suggesting FGF21  
398 resistance (Fisher et al., 2010). FGF21-null mice are more prone to developing NASH,  
399 have decreased PGC1 $\alpha$  expression, reduced hepatic FA activation and beta-oxidation  
400 (Fisher et al., 2014; Liu et al., 2016; Potthoff et al., 2009).

401

402 Pharmacological administration of FGF21 analogues reduces hepatic fat content,  
403 inflammation and fibrosis in mice and humans (Coskun et al., 2008; Sanyal et al., 2019), by  
404 inducing PGC1 $\alpha$  and its downstream genes, *CPT1A*, *CPT1B*, and promoting hepatic FA  
405 oxidation (Fisher et al., 2014; Keinicke et al., 2020). PGC1 $\alpha$  regulates energy homeostasis  
406 and mitochondrial number and function (Piccini et al. 2018). PGC1 $\alpha$  overexpression results  
407 in increased fatty acid oxidation and decreased hepatic triglyceride content (Morris et al.,  
408 2012) while PGC1 $\alpha$  deficiency results in decreased lipid oxidation and hepatic steatosis  
409 (Estall et al., 2009; Leone et al. 2005). Decreased expression of genes involved in rate  
410 limiting mitochondrial transport of FA for beta oxidation, peroxisomal beta oxidation and  
411 omega oxidation combined with increased hepatic triglycerides in adolescent female PA  
412 sheep may therefore be a consequence of decreased expression of *FGF21* and

413 *PPARGC1A*, further supported by our observation of positive correlation between hepatic  
414 *PPARGC1A* expression and genes involved in lipid oxidation.

415

416 In addition to its metabolic function, PGC1 $\alpha$  protects against inflammation, decreasing  
417 expression of pro-inflammatory cytokines and stimulating expression of anti-inflammatory  
418 factors (Leveille et al., 2020). In animal models reduced levels of PGC1 $\alpha$  potentiate  
419 progression of NAFLD to NASH and increase pro-inflammatory environment in liver tissue  
420 (Besse-Patin et al., 2017) while FGF21 deficiency results in increased hepatic macrophage  
421 infiltration, augmented inflammation with elevated expression of pro-inflammatory and pro-  
422 fibrotic cytokines (Liu et al., 2016; Zheng et al., 2020), whilst gene therapy increasing  
423 hepatic FGF21 synthesis inhibits macrophage infiltration, inflammation and fibrosis  
424 (Jimenez et al., 2018). Pharmacological administration of FGF21 in animal models of  
425 hepatic injury, alcoholic and non-alcoholic steatosis decreases hepatic expression of  
426 molecular markers of pro-inflammatory macrophages, *CD68*, *F4/80* (encoded by *ADGRE1*),  
427 and pro-inflammatory cytokines, including *IL1B* and *TNF* (Bao et al., 2018; Cui et al., 2020;  
428 Lee et al., 2016). We have observed herein that adolescent PA sheep had increased  
429 mRNA expression of markers of pro-inflammatory macrophages, *CD68*, *ADGRE1* (coding  
430 for *F4/80*), *TLR2* and *TLR4*, pro-inflammatory cytokines *IL1B* and *IL18* and chemokines  
431 *CXCL9*, *CXCL10* and *CCL5*. Again, our data appears in agreement with studies on FGF21  
432 and PGC1 $\alpha$  deficiency animal models.

433

434 In conclusion, based on evidence presented using realistic clinical model of PCOS,  
435 targeting FGF21 expression during adolescence may be a potential therapeutic option to  
436 prevent onset of adipocyte and liver dysfunction, and thus sidestep the subsequent serious  
437 health relevant consequences associated with PCOS.



439 **Acknowledgements**

440 The authors wish to acknowledge Joan Docherty, John Hogg, Marjorie Thomson, Peter  
441 Tennant and James Nixon and the staff at the Marshall Building, University of Edinburgh for  
442 their excellent animal husbandry. Dr Kirsten Hogg, Dr Fiona Connolly, Dr Junko Nio-  
443 Kobayashi, Dr Avi Lerner and Lyndsey Boswell helped with tissue collection.

444

445 **Funding**

446 This work was funded by Medical Research Council (MRC) project grants (G0500717;  
447 G0801807; G0802782; MR/P011535/1) and supported by the MRC Centre for Reproductive  
448 Health (MR/N022556/1).

449

450 **Declaration of interest**

451 The authors have no conflicts of interest to declare.

452

453 **References**

454 Adams, A.C., Cheng, C.C., Coskun, T., Kharitononkov, A., 2012a. FGF21 requires  $\beta$ klotho  
455 to act in vivo. PLoS ONE 7, e49977. doi:10.1371/journal.pone.0049977

456

457 Adams, A.C., Yang, C., Coskun, T., Cheng, C.C., Gimeno, R.E., Luo, Y., Kharitononkov, A.,  
458 2012b. The breadth of FGF21's metabolic actions are governed by FGFR1 in adipose  
459 tissue. Mol. Metab. 2, 31–37. doi:10.1016/j.molmet.2012.08.007

460

461 Alisi, A., Ceccarelli, S., Panera, N., Prono, F., Petrini, S., De Stefanis, C., Pezzullo, M.,  
462 Tozzi, A., Villani, A., Bedogni, G., Nobili, V., 2013. Association between Serum Atypical  
463 Fibroblast Growth Factors 21 and 19 and Pediatric Nonalcoholic Fatty Liver Disease. PLoS  
464 ONE 8, e67160. doi:10.1371/journal.pone.0067160

465

466 Ayonrinde, O.T., Adams, L.A., Doherty, D.A., Mori, T.A., Beilin, L.J., Oddy, W.H., Hickey,  
467 M., Sloboda, D.M., Olynyk, J.K., Hart, R., 2016. Adverse metabolic phenotype of  
468 adolescent girls with non-alcoholic fatty liver disease plus polycystic ovary syndrome  
469 compared with other girls and boys. J. Gastroenterol. Hepatol. 31, 980–987.  
470 doi:10.1111/jgh.13241

471

472 Badman, M.K., Koester, A., Flier, J.S., Kharitononkov, A., Maratos-Flier, E., 2009.  
473 Fibroblast growth factor 21-deficient mice demonstrate impaired adaptation to ketosis.  
474 Endocrinology 150, 4931–4940. doi:10.1210/en.2009-0532

475

476 Bao, L., Yin, J., Gao, W., Wang, Q., Yao, W., Gao, X., 2018. A long-acting FGF21 alleviates  
477 hepatic steatosis and inflammation in a mouse model of non-alcoholic steatohepatitis partly

478 through an FGF21-adiponectin-IL17A pathway. *Br. J. Pharmacol.* 175, 3379–3393.  
479 doi:10.1111/bph.14383  
480

481 Barb, D., Bril, F., Kalavalapalli, S., Cusi, K., 2019. Plasma Fibroblast Growth Factor 21 Is  
482 Associated With Severity of Nonalcoholic Steatohepatitis in Patients With Obesity and Type  
483 2 Diabetes. *J. Clin. Endocrinol. Metab.* 104, 3327–3336. doi:10.1210/jc.2018-02414  
484

485 Barrett, E.S., Hoeger, K.M., Sathyanarayana, S., Abbott, D.H., Redmon, J.B., Nguyen,  
486 R.H.N., Swan, S.H., 2018. Anogenital distance in newborn daughters of women with  
487 polycystic ovary syndrome indicates fetal testosterone exposure. *J. Dev. Orig. Health Dis.*  
488 9, 307-314. doi: 10.1017/S2040174417001118.  
489

490 Besse-Patin, A., Léveillé, M., Oropeza, D., Nguyen, B.N., Prat, A., Estall, J.L., 2017.  
491 Estrogen Signals Through Peroxisome Proliferator-Activated Receptor- $\gamma$  Coactivator 1 $\alpha$  to  
492 Reduce Oxidative Damage Associated With Diet-Induced Fatty Liver Disease.  
493 *Gastroenterology.* 152, 243-256. doi: 10.1053/j.gastro.2016.09.017.  
494

495 Bisgaard, A., Sorensen, K., Johannsen, T.H., Helge, J.W., Andersson, A.-M., Juul, A.,  
496 2014. Significant gender difference in serum levels of fibroblast growth factor 21 in Danish  
497 children and adolescents. *Int. J. Pediatr. Endocrinol.* 2014, 7. doi:10.1186/1687-9856-2014-  
498 7  
499

500 Booth, A., Magnuson, A., Foster, M., 2014. Detrimental and protective fat: body fat  
501 distribution and its relation to metabolic disease. *Horm. Mol. Biol. Clin. Investig.* 17, 13–27.  
502 doi:10.1515/hmbci-2014-0009



503

504 Cankaya, S., Demir, B., Aksakal, S.E., Dilbaz, B., Demirtas, C., Goktolga, U., 2014. Insulin  
505 resistance and its relationship with high molecule weight adiponectin in adolescents with  
506 polycystic ovary syndrome and a maternal history. *Fertil. Steril.* 102, 826–830.  
507 doi:10.1016/j.fertnstert.2014.05.032

508

509 Connolly, F., Rae, M.T., Butler, M., Klibanov, A.L., Sboros, V., McNeilly, A.S., Duncan,  
510 W.C., 2014. The local effects of ovarian diathermy in an ovine model of polycystic ovary  
511 syndrome. *PLoS One.* 9, e111280. doi: 10.1371/journal.pone.0111280.

512

513 Coskun, T., Bina, H.A., Schneider, M.A., Dunbar, J.D., 2008. Fibroblast growth factor 21  
514 corrects obesity in mice. *Endocrinology* 149, 6018-6027. doi:10.1210/en.2008-0816

515

516 Cui, A., Li, J., Ji, S., Ma, F., Wang, G., Xue, Y., Liu, Z., Gao, J., Han, J., Tai, P., Wang, T.,  
517 Chen, J., Ma, X., Li, Y., 2020. The Effects of B1344, a Novel Fibroblast Growth Factor 21  
518 Analog, on Nonalcoholic Steatohepatitis in Nonhuman Primates. *Diabetes* 69, 1611–1623.  
519 doi:10.2337/db20-0209

520

521 Daan, N.M., Koster, M.P., Steegers-Theunissen, R.P., Eijkemans, M.J., Fauser, B.C., 2017.  
522 Endocrine and cardiometabolic cord blood characteristics of offspring born to mothers with  
523 and without polycystic ovary syndrome. *Fertil Steril.* 107, 261-268.e3. doi:  
524 10.1016/j.fertnstert.2016.09.042.

525

526 Ding, X., Boney-Montoya, J., Owen, B.M., Bookout, A.L., Coate, K.C., Mangelsdorf, D.J.,  
527 Kliewer, S.A., 2012.  $\beta$ Klotho is required for fibroblast growth factor 21 effects on growth and  
528 metabolism. *Cell Metab.* 16, 387–393. doi:10.1016/j.cmet.2012.08.002  
529

530 Dushay, J., Chui, P.C., Gopalakrishnan, G.S., Varela-Rey, M., Crawley, M., Fisher, F.M.,  
531 Badman, M.K., Martinez-Chantar, M.L., Maratos-Flier, E., 2010. Increased fibroblast growth  
532 factor 21 in obesity and nonalcoholic fatty liver disease. *Gastroenterology* 139, 456–463.  
533 doi:10.1053/j.gastro.2010.04.054  
534

535 Dutchak, P.A., Katafuchi, T., Bookout, A.L., Choi, J.H., Yu, R.T., Mangelsdorf, D.J., Kliewer,  
536 S.A., 2012. Fibroblast growth factor-21 regulates PPAR $\gamma$  activity and the antidiabetic  
537 actions of thiazolidinediones. *Cell* 148, 556–567. doi:10.1016/j.cell.2011.11.062  
538

539 Echiburú, B., Pérez-Bravo, F., Galgani, J.E., Sandoval, D., Saldías, C., Crisosto, N.,  
540 Maliqueo, M., Sir-Petermann, T., 2018. Enlarged adipocytes in subcutaneous adipose  
541 tissue associated to hyperandrogenism and visceral adipose tissue volume in women with  
542 polycystic ovary syndrome. *Steroids* 130, 15–21. doi:10.1016/j.steroids.2017.12.009  
543

544 Escobar-Morreale, H.F., Villuendas, G., Botella-Carretero, J.I., Álvarez-Blasco, F.,  
545 Sanchón, R., Luque-Ramírez, M., Millán, J.L.S., 2006. Adiponectin and resistin in PCOS: a  
546 clinical, biochemical and molecular genetic study. *Hum. Reprod.* 21, 2257–2265.  
547 doi:10.1093/humrep/del146  
548

549 Estall, J.L., Kahn, M., Cooper, M.P., Fisher, F.M., Wu, M.K., Laznik, D., Qu, L., Cohen,  
550 D.E., Shulman, G.I., Spiegelman, B.M., 2009. Sensitivity of lipid metabolism and insulin

551 signaling to genetic alterations in hepatic peroxisome proliferator-activated receptor-gamma  
552 coactivator-1alpha expression. *Diabetes*. 58, 1499-508. doi: 10.2337/db08-1571.

553

554 Fauser B.C., Tarlatzis B.C., Rebar R.W., Legro R.S., Balen A.H., Lobo R., Carmina E.,  
555 Chang J., Yildiz B.O., Laven J.S.E. *et al.* 2012 Consensus on women's health aspects of  
556 polycystic ovary syndrome (PCOS): the Amsterdam ESHRE/ASRM-Sponsored 3rd PCOS  
557 Consensus Workshop Group. *Hum. Reprod.* 27, 14-24. doi: 10.1093/humrep/der396

558

559 Fazel, Y., Koenig, A.B., Sayiner, M., Goodman, Z.D., Younossi, Z.M., 2016. Epidemiology  
560 and natural history of non-alcoholic fatty liver disease. *Metabolism* 65, 1017–1025.  
561 doi:10.1016/j.metabol.2016.01.012

562

563 Fisher, F.M., Chui, P.C., Antonellis, P.J., Bina, H.A., Kharitononkov, A., Flier, J.S., Maratos-  
564 Flier, E., 2010. Obesity is a fibroblast growth factor 21 (FGF21)-resistant state. *Diabetes* 59,  
565 2781–2789. doi:10.2337/db10-0193

566

567 Fisher, F.M., Chui, P.C., Nasser, I.A., Popov, Y., Cunniff, J.C., Lundasen, T.,  
568 Kharitononkov, A., Schuppan, D., Flier, J.S., Maratos-Flier, E., 2014. Fibroblast Growth  
569 Factor 21 Limits Lipotoxicity by Promoting Hepatic Fatty Acid Activation in Mice on  
570 Methionine and Choline-Deficient Diets. *Gastroenterology* 147, 1073–1083.e6.  
571 doi:10.1053/j.gastro.2014.07.044

572

573 Fisher, F.M., Maratos-Flier, E., 2016. Understanding the Physiology of FGF21. *Annu. Rev.*  
574 *Physiol.* 78, 223–241. doi:10.1146/annurev-physiol-021115-105339

575

576 Gaich, G., Chien, J.Y., Fu, H., Glass, L.C., Deeg, M.A., Holland, W.L., Kharitonov, A.,  
577 Bumol, T., Schilske, H.K., Moller, D.E., 2013. The effects of LY2405319, an FGF21 analog,  
578 in obese human subjects with type 2 diabetes. *Cell Metab.* 18, 333–340.  
579 doi:10.1016/j.cmet.2013.08.005  
580  
581 Gao, B., Tsukamoto, H., 2016. Inflammation in Alcoholic and Nonalcoholic Fatty Liver  
582 Disease: Friend or Foe?. *Gastroenterology.* 150, 1704-1709.  
583 doi:10.1053/j.gastro.2016.01.025  
584  
585 Gorar, S., Culha, C., Uc, Z.A., Dellal, F.D., Serter, R., Aral, S., Aral, Y., 2010. Serum  
586 fibroblast growth factor 21 levels in polycystic ovary syndrome. *Gynecol. Endocrinol.* 26,  
587 819–826. doi:10.3109/09513590.2010.487587  
588  
589 Hanssen, M.J.W., Broeders, E., Samms, R.J., Vosselman, M.J., van der Lans, A.A.J.J.,  
590 Cheng, C.C., Adams, A.C., van Marken Lichtenbelt, W.D., Schrauwen, P., 2015. Serum  
591 FGF21 levels are associated with brown adipose tissue activity in humans. *Sci. Rep.* 5,  
592 10275. doi:10.1038/srep10275  
593  
594 Hogg, K., Wood, C., McNeilly, A.S., Duncan, W.C., 2011. The in utero programming effect  
595 of increased maternal androgens and a direct fetal intervention on liver and metabolic  
596 function in adult sheep. *PLoS ONE* 6, e24877. doi:10.1371/journal.pone.0024877  
597  
598 Hogg, K., Young, J.M., Oliver, E.M., Souza, C.J., McNeilly, A.S., Duncan, W.C., 2012.  
599 Enhanced Thecal Androgen Production Is Prenatally Programmed in an Ovine Model of  
600 Polycystic Ovary Syndrome. *Endocrinology* 153, 450–461. doi:10.1210/en.2011-1607

601

602 Holland, W.L., Adams, A.C., Brozinick, J.T., Bui, H.H., Miyauchi, Y., Kusminski, C.M.,  
603 Bauer, S.M., Wade, M., Singhal, E., Cheng, C.C., Volk, K., Kuo, M.-S., Gordillo, R.,  
604 Kharitononkov, A., Scherer, P.E., 2013. An FGF21-adiponectin-ceramide axis controls  
605 energy expenditure and insulin action in mice. *Cell Metab.* 17, 790–797.  
606 doi:10.1016/j.cmet.2013.03.019

607

608 Jason, J., 2011. Polycystic ovary syndrome in the United States: clinical visit rates,  
609 characteristics, and associated health care costs. *Arch. Intern. Med.* 171, 1209–1211.  
610 doi:10.1001/archinternmed.2011.288

611

612 Jimenez, V., Jambrina, C., Casana, E., Sacristan, V., Muñoz, S., Darriba, S., Rodó, J.,  
613 Mallol, C., Garcia, M., León, X., Marcó, S., Ribera, A., Elias, I., Casellas, A., Grass, I., Elias,  
614 G., Ferré, T., Motas, S., Franckhauser, S., Mulero, F., Navarro, M., Haurigot, V., Ruberte,  
615 J., Bosch, F., 2018. FGF21 gene therapy as treatment for obesity and insulin resistance.  
616 *EMBO Mol. Med.* 10, 21. doi:10.15252/emmm.201708791

617

618 Keinicke, H., Sun, G., Mentzel, C.M.J., Fredholm, M., John, L.M., Andersen, B., Raun, K.,  
619 Kjaergaard, M., 2020. FGF21 regulates hepatic metabolic pathways to improve steatosis  
620 and inflammation. *Endocr. Connect.* 9, 755–768. doi:10.1530/EC-20-0152

621

622 Kharitononkov, A., Shiyanova, T.L., Koester, A., Ford, A.M., Micanovic, R., Galbreath, E.J.,  
623 Sandusky, G.E., Hammond, L.J., Moyers, J.S., Owens, R.A., Gromada, J., Brozinick, J.T.,  
624 Hawkins, E.D., Wroblewski, V.J., Li, D.-S., Mehrbod, F., Jaskunas, S.R., Shanafelt, A.B.,

625 2005. FGF-21 as a novel metabolic regulator. *J. Clin. Invest.* 115, 1627–1635.  
626 doi:10.1172/JCI23606  
627  
628 Kharitononkov, A., Wroblewski, V.J., Koester, A., Chen, Y.-F., Clutinger, C.K., Tigno, X.T.,  
629 Hansen, B.C., Shanafelt, A.B., Etgen, G.J., 2007. The metabolic state of diabetic monkeys  
630 is regulated by fibroblast growth factor-21. *Endocrinology* 148, 774–781.  
631 doi:10.1210/en.2006-1168  
632  
633 Lee, J.H., Kang, Y.E., Chang, J.Y., Park, K.C., Kim, H.-W., Kim, J.T., Kim, H.J., Yi, H.-S.,  
634 Shong, M., Chung, H.K., Kim, K.S., 2016. An engineered FGF21 variant, LY2405319, can  
635 prevent non-alcoholic steatohepatitis by enhancing hepatic mitochondrial function. *Am. J.*  
636 *Transl. Res.* 8, 4750–4763.  
637  
638 Leone, T.C., Lehman, J.J., Finck, B.N., Schaeffer, P.J., Wende, A.R., Boudina, S., Courtois,  
639 M., Wozniak, D.F., Sambandam, N., Bernal-Mizrachi, C., Chen, Z., Holloszy, J.O.,  
640 Medeiros, D.M., Schmidt, R.E., Saffitz, J.E., Abel, E.D., Semenkovich, C.F., Kelly, D.P.,  
641 2005. PGC-1alpha deficiency causes multi-system energy metabolic derangements:  
642 Muscle dysfunction, abnormal weight control and hepatic steatosis. *PLoS Biol.* 3, 672-687.  
643 doi: 10.1371/journal.pbio.0030101  
644  
645 Léveillé, M., Besse-Patin, A., Jouvét, N., Gunes, A., Sczelecki, S., Jeromson, S., Khan,  
646 N.P., Baldwin, C., Dumouchel, A., Correia, J.C., Jannig, P.R., Boulais, J., Ruas, J.L., Estall,  
647 J.L., 2020. PGC-1 $\alpha$  isoforms coordinate to balance hepatic metabolism and apoptosis in  
648 inflammatory environments. *Mol Metab.* 34, 72-84. doi: 10.1016/j.molmet.2020.01.004.  
649

650 Lewis, J.E., Ebling, F.J.P., Samms, R.J., Tsintzas, K., 2019. Going Back to the Biology of  
651 FGF21: New Insights. *Trends Endocrinol. Metab.* 30, 491–504.  
652 doi:10.1016/j.tem.2019.05.007  
653

654 Li, G., Yin, J., Fu, J., Li, L., Grant, S.F.A., Li, C., Li, M., Mi, J., Gao, S., 2017. FGF21  
655 deficiency is associated with childhood obesity, insulin resistance and  
656 hypoadiponectinaemia: The BCAMS Study. *Diabetes Metab.* 43, 253–260.  
657 doi:10.1016/j.diabet.2016.12.003  
658

659 Li, H., Wu, G., Fang, Q., Zhang, M., Hui, X., Sheng, B., Wu, L., Bao, Y., Li, P., Xu, A., Jia,  
660 W., 2018. Fibroblast growth factor 21 increases insulin sensitivity through specific  
661 expansion of subcutaneous fat. *Nat. Commun.* 9, 272–16. doi:10.1038/s41467-017-02677-  
662 9  
663

664 Lin, Y.C., Chang, P.F., Chang, M.H., Ni, Y.H., 2013. A common variant in the peroxisome  
665 proliferator-activated receptor- $\gamma$  coactivator-1 $\alpha$  gene is associated with nonalcoholic fatty  
666 liver disease in obese children. *Am. J. Clin. Nutr.* 97, 326-331. doi:  
667 10.3945/ajcn.112.046417.  
668

669 Lin, Z., Tian, H., Lam, K.S.L., Lin, S., Hoo, R.C.L., Konishi, M., Itoh, N., Wang, Y.,  
670 Bornstein, S.R., Xu, A., Li, X., 2013. Adiponectin mediates the metabolic effects of FGF21  
671 on glucose homeostasis and insulin sensitivity in mice. *Cell Metab.* 17, 779–789.  
672 doi:10.1016/j.cmet.2013.04.005  
673

674 Liu, X., Zhang, P., Martin, R.C., Cui, G., Wang, G., Tan, Y., Cai, L., Lv, G., Li, Y., 2016.  
675 Lack of fibroblast growth factor 21 accelerates metabolic liver injury characterized by  
676 steatohepatities in mice. *Am. J. Cancer Res.* 6, 1011–1025.  
677  
678 Livak, K.J., Schmittgen, T.D., 2001. Analysis of Relative Gene Expression Data Using Real-  
679 Time Quantitative PCR and the  $2^{-\Delta\Delta CT}$  Method. *Methods* 25, 402–408.  
680 doi:10.1006/meth.2001.1262  
681  
682 Maliqueo, M., Maliqueo, M., Pérez-Bravo, F., Galgani, J.E., Galgani, J.E., Pérez, F.,  
683 Echiburú, B., Echiburú, B., Crisosto, N., de Guevara, A.L., Sir-Petermann, T., 2012.  
684 Relationship of serum adipocyte-derived proteins with insulin sensitivity and reproductive  
685 features in pre-pubertal and pubertal daughters of polycystic ovary syndrome women. *Eur.*  
686 *J. Obstet. Gynecol. Reprod. Biol.* 161, 56–61. doi:10.1016/j.ejogrb.2011.12.012  
687  
688 Manneras-Holm, L., Leonhardt, H., Jennische, E., Kullberg, J., Oden, A., Holm, G.,  
689 Hellstrom, M., Lonn, L., Olivecrona, G., Stener-Victorin, E., Lonn, M., 2010. Adipose tissue  
690 has aberrant morphology and function in PCOS: enlarged adipocytes and low serum  
691 adiponectin, but not circulating sex steroids, are strongly associated with insulin resistance.  
692 *J. Clin. Endocrinol. Metab.* 96, E304–11. doi:10.1210/jc.2010-1290  
693  
694 Moran, L.J., Teede, H.J., Norman, R.J., 2015. Metabolic risk in PCOS: phenotype and  
695 adiposity impact. *Trends Endocrinol. Metab.* 26, 136–143. doi:10.1016/j.tem.2014.12.003  
696 Paschou, S.A., Polyzos, S.A., Anagnostis, P., Goulis, D.G., Kanaka-Gantenbein, C.,  
697 Lambrinoudaki, I., Georgopoulos, N.A., Vryonidou, A., 2020. Nonalcoholic fatty liver



698 disease in women with polycystic ovary syndrome. *Endocrine* 67, 1–8. doi:10.1007/s12020-  
699 019-02085-7

700

701 Morris, E.M., Meers, G.M., Booth, F.W., Fritsche, K.L., Hardin, C.D., Thyfault, J.P., Ibdah,  
702 J.A., 2012. PGC-1 $\alpha$  overexpression results in increased hepatic fatty acid oxidation with  
703 reduced triacylglycerol accumulation and secretion. *Am. J. Physiol. Gastrointest. Liver*  
704 *Physiol.* 303, G979-G992. doi:10.1152/ajpgi.00169.2012

705

706 Oates, J.R., McKell M.C., Moreno-Fernandez M.E., Damen M.S.M.A., Deepe G.S., Qualls  
707 J.E., Divanovic S., 2019. Macrophage Function in the Pathogenesis of Non-alcoholic Fatty  
708 Liver Disease: The Mac Attack. *Front Immunol.* 10, 2893. doi:10.3389/fimmu.2019.02893

709

710 Padmanabhan, V., Veiga-Lopez, A., 2013. Sheep models of polycystic ovary syndrome  
711 phenotype. *Mol. Cell. Endocrinol.* 373, 8-20. doi:10.1016/j.mce.2012.10.005

712 Piccinin, E., Villani, G., Moschetta, A., 2018. Metabolic aspects in NAFLD, NASH and  
713 hepatocellular carcinoma: the role of PGC1 coactivators. *Nat. Rev. Gastroenterol. Hepatol.*  
714 16,160–174. doi:10.1038/s41575-018-0089-3

715

716 Potthoff, M.J., Inagaki, T., Satapati, S., Ding, X., He, T., Goetz, R., Mohammadi, M., Finck,  
717 B.N., Mangelsdorf, D.J., Kliewer, S.A., Burgess, S.C., 2009. FGF21 induces PGC-1 $\alpha$  and  
718 regulates carbohydrate and fatty acid metabolism during the adaptive starvation response.  
719 *Proc. Nat. Acad. Sci.* 106, 10853–10858. doi:10.1073/pnas.0904187106

720

721 Puder, J.J., Varga, S., Kraenzlin, M., De Geyter, C., Keller, U., Müller, B., 2005. Central fat  
722 excess in polycystic ovary syndrome: relation to low-grade inflammation and insulin  
723 resistance. *J. Clin. Endocrinol. Metab.* 90, 6014–6021. doi:10.1210/jc.2005-1002  
724

725 Rae, M., Grace, C., Hogg, K., Wilson, L.M., McHaffie, S.L., Ramaswamy, S., MacCallum,  
726 J., Connolly, F., McNeilly, A.S., Duncan, C., 2013. The pancreas is altered by in utero  
727 androgen exposure: implications for clinical conditions such as polycystic ovary syndrome  
728 (PCOS). *PLoS ONE* 8, e56263. doi:10.1371/journal.pone.0056263  
729

730 Ramaswamy, S., Grace, C., Mattei, A.A., Siemienowicz, K., Brownlee, W., MacCallum, J.,  
731 McNeilly, A.S., Duncan, W.C., Rae, M.T., 2016. Developmental programming of polycystic  
732 ovary syndrome (PCOS): prenatal androgens establish pancreatic islet  $\alpha/\beta$  cell ratio and  
733 subsequent insulin secretion. *Sci. Rep.* 6, 27408. doi:10.1038/srep27408  
734

735 Risal, S., Pei, Y., Lu, H., Manti, M., Fornes, R., Pui, H.P., Zhao, Z., Massart, J., Ohlsson,  
736 C., Lindgren, E., Crisosto, N., Maliqueo, M., Echiburú, B., Ladrón de Guevara, A., Sir-  
737 Petermann, T., Larsson, H., Rosenqvist, M.A., Cesta, C.E., Benrick, A., Deng, Q., Stener-  
738 Victorin, E., 2019. Prenatal androgen exposure and transgenerational susceptibility to  
739 polycystic ovary syndrome. *Nat Med.* 25, 1894-1904. doi: 10.1038/s41591-019-0666-1.  
740

741 Sahin, S.B., Ayaz, T., Cure, M.C., Sezgin, H., Ural, U.M., Balik, G., Sahin, F.K., 2014.  
742 Fibroblast growth factor 21 and its relation to metabolic parameters in women with  
743 polycystic ovary syndrome. *Scand. J. Clin. Lab. Invest.* 74, 465–469.  
744 doi:10.3109/00365513.2014.900821  
745

746 Sanyal, A., Charles, E.D., Neuschwander-Tetri, B.A., Loomba, R., Harrison, S.A.,  
747 Abdelmalek, M.F., Lawitz, E.J., Halegoua-DeMarzio, D., Kundu, S., Noviello, S., Luo, Y.,  
748 Christian, R., 2019. Pegbelfermin (BMS-986036), a PEGylated fibroblast growth factor 21  
749 analogue, in patients with non-alcoholic steatohepatitis: a randomised, double-blind,  
750 placebo-controlled, phase 2a trial. *Lancet* 392, 2705–2717. doi:10.1016/S0140-  
751 6736(18)31785-9  
752  
753 Sarkar, M., Terrault, N., Chan, W., Cedars, M.I., Huddleston, H.G., Duwaerts, C.C.,  
754 Balitzer, D., Gill, R.M., 2020. Polycystic ovary syndrome (PCOS) is associated with NASH  
755 severity and advanced fibrosis. *Liver Int.* 40, 355–359. doi:10.1111/liv.14279  
756  
757 Siemienowicz, K., Rae, M.T., Howells, F., Anderson, C., Nicol, L.M., Franks, S., Duncan,  
758 W.C., 2020. Insights into manipulating postprandial energy expenditure to manage weight  
759 gain in polycystic ovary syndrome (PCOS). *iScience* 101164.  
760 doi:10.1016/j.isci.2020.101164  
761  
762 Siemienowicz, K.J., Coukan, F., Franks, S., Rae, M.T., Duncan, W.C., 2021. Aberrant  
763 subcutaneous adipogenesis precedes adult metabolic dysfunction in an ovine model of  
764 polycystic ovary syndrome (PCOS). *Mol. Cell. Endocrinol.* 519, 111042.  
765 doi:10.1016/j.mce.2020.111042  
766 Siemienowicz, K.J., Filis, P., Shaw, S., Douglas, A., Thomas, J., Mulroy, S., Howie, F.,  
767 Fowler, P.A., Duncan, W.C., Rae, M.T., 2019. Fetal androgen exposure is a determinant of  
768 adult male metabolic health. *Sci. Rep.* 9, 20195–17. doi:10.1038/s41598-019-56790-4  
769

770 So, W.Y., Cheng, Q., Xu, A., Lam, K.S.L., Leung, P.S., 2015. Loss of fibroblast growth  
771 factor 21 action induces insulin resistance, pancreatic islet hyperplasia and dysfunction in  
772 mice. *Cell Death Dis* 6, e1707. doi:10.1038/cddis.2015.80  
773

774 Talukdar, S., Zhou, Y., Li, D., Rossulek, M., Dong, J., Somayaji, V., Weng, Y., Clark, R.,  
775 Lanba, A., Owen, B.M., Brenner, M.B., Trimmer, J.K., Gropp, K.E., Chabot, J.R., Erion,  
776 D.M., Rolph, T.P., Goodwin, B., Calle, R.A., 2016. A Long-Acting FGF21 Molecule, PF-  
777 05231023, Decreases Body Weight and Improves Lipid Profile in Non-human Primates and  
778 Type 2 Diabetic Subjects. *Cell Metab.* 23, 427–440. doi:10.1016/j.cmet.2016.02.001  
779

780 Tanaka, N., Takahashi, S., Zhang, Y., Krausz, K.W., Smith, P.B., Patterson, A.D.,  
781 Gonzalez, F.J., 2015. Role of fibroblast growth factor 21 in the early stage of NASH induced  
782 by methionine- and choline-deficient diet. *Biochim. Biophys. Acta* 1852, 1242–1252.  
783 doi:10.1016/j.bbadis.2015.02.012  
784

785 Teede, H., Deeks, A., Moran, L., 2010. Polycystic ovary syndrome: a complex condition  
786 with psychological, reproductive and metabolic manifestations that impacts on health  
787 across the lifespan. *BMC Med.* 8, 41. doi:10.1186/1741-7015-8-41  
788

789 Véniant, M.M., Hale, C., Helmering, J., Chen, M.M., Stanislaus, S., Busby, J., Vonderfecht,  
790 S., Xu, J., Lloyd, D.J., 2012. FGF21 promotes metabolic homeostasis via white adipose and  
791 leptin in mice. *PLoS ONE* 7, e40164. doi:10.1371/journal.pone.0040164  
792

793 Westerbacka, J., Kolak, M., Kiviluoto, T., Arkkila, P., Sirén, J., Hamsten, A., Fisher, R.M.,  
794 Yki-Järvinen, H., 2007. Genes involved in fatty acid partitioning and binding, lipolysis,

795 monocyte/macrophage recruitment, and inflammation are overexpressed in the human fatty  
796 liver of insulin-resistant subjects. *Diabetes*. 56, 2759-65. doi: 10.2337/db07-0156.

797

798 Xu, J., Lloyd, D.J., Hale, C., Stanislaus, S., Chen, M., Sivits, G., Vonderfecht, S., Hecht, R.,  
799 Li, Y.-S., Lindberg, R.A., Chen, J.-L., Jung, D.Y., Zhang, Z., Ko, H.-J., Kim, J.K., Véniant,  
800 M.M., 2009a. Fibroblast growth factor 21 reverses hepatic steatosis, increases energy  
801 expenditure, and improves insulin sensitivity in diet-induced obese mice. *Diabetes* 58, 250–  
802 259. doi:10.2337/db08-0392

803

804 Xu, J., Stanislaus, S., Chinookoswong, N., Lau, Y.Y., Hager, T., Patel, J., Ge, H.,  
805 Weizmann, J., Lu, S.-C., Graham, M., Busby, J., Hecht, R., Li, Y.-S., Li, Y., Lindberg, R.,  
806 Véniant, M.M., 2009b. Acute glucose-lowering and insulin-sensitizing action of FGF21 in  
807 insulin-resistant mouse models--association with liver and adipose tissue effects. *Am. J.*  
808 *Physiol. Endocrinol.* 297, E1105–14. doi:10.1152/ajpendo.00348.2009

809

810 Yang, C., Jin, C., Li, X., Wang, F., McKeehan, W.L., Luo, Y., 2012. Differential specificity of  
811 endocrine FGF19 and FGF21 to FGFR1 and FGFR4 in complex with KLB. *PLoS ONE* 7,  
812 e33870. doi:10.1371/journal.pone.0033870

813

814 Ye, D., Wang, Y., Li, H., Jia, W., Man, K., Lo, C.M., Wang, Y., Wang, Y., Lam, K.S.L., Xu,  
815 A., 2014. Fibroblast growth factor 21 protects against acetaminophen-induced  
816 hepatotoxicity by potentiating peroxisome proliferator-activated receptor coactivator protein-  
817 1 $\alpha$ -mediated antioxidant capacity in mice. *Hepatology* 60, 977–989. doi:10.1002/hep.27060

818

819 Yildirim, B., Sabir, N., Sabir, Kaleli, B., 2003. Relation of intra-abdominal fat distribution to  
820 metabolic disorders in nonobese patients with polycystic ovary syndrome. *Fertil. Steril.* 79,  
821 1358–1364. doi:10.1016/S0015-0282(03)00265-6  
822

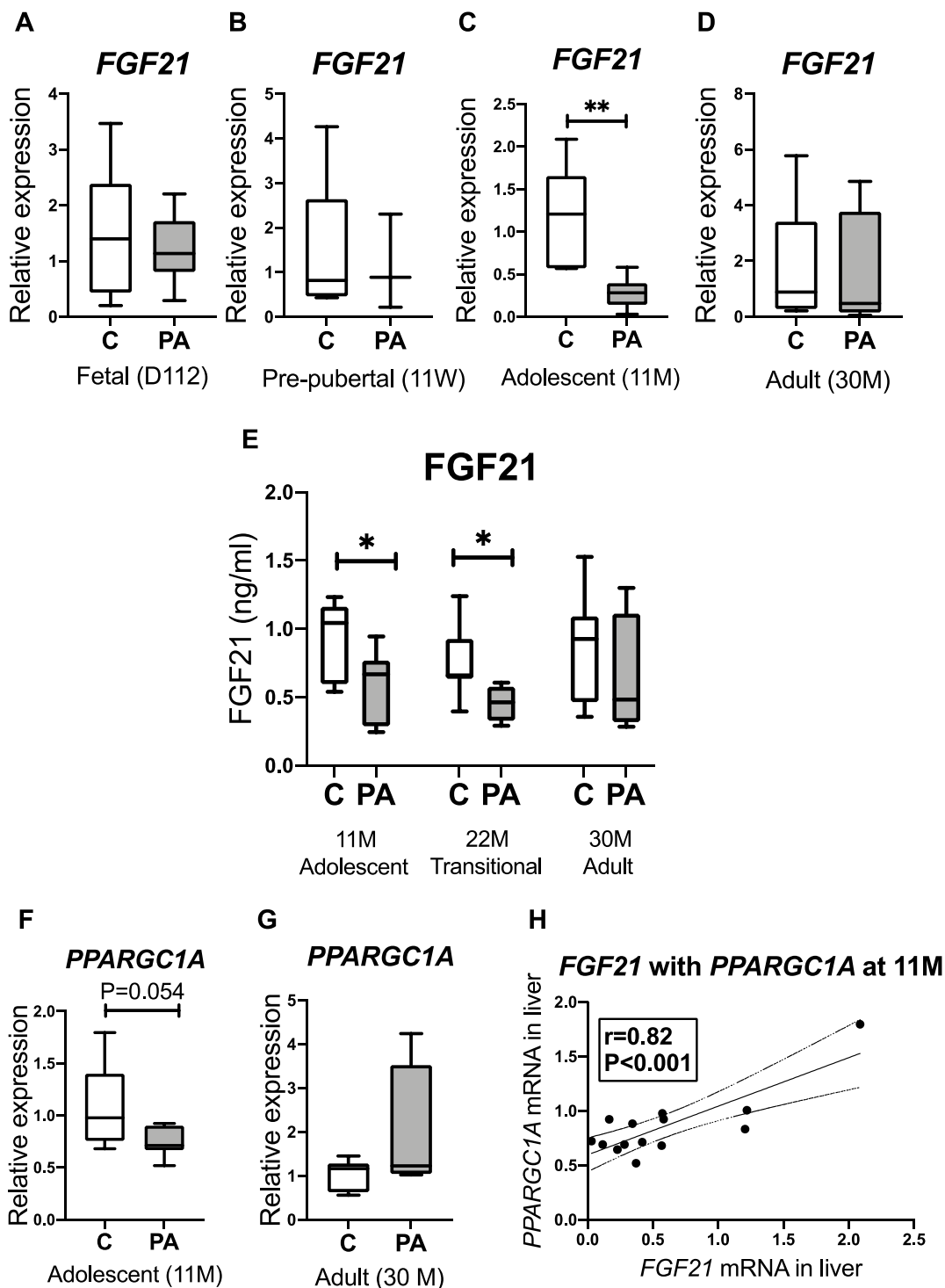
823 Yoneda, M., Hotta, K., Nozaki, Y., Endo, H., Uchiyama, T., Mawatari, H., Iida, H., Kato, S.,  
824 Hosono, K., Fujita, K., Yoneda, K., Takahashi, H., Kirikoshi, H., Kobayashi, N., Inamori, M.,  
825 Abe, Y., Kubota, K., Saito, S., Maeyama, S., Wada, K., Nakajima, A., 2008. Association  
826 between PPARGC1A polymorphisms and the occurrence of nonalcoholic fatty liver disease  
827 (NAFLD). *BMC Gastroenterol.* 8, 27. doi: 10.1186/1471-230X-8-27.  
828

829 Zarei, M., Pizarro-Delgado, J., Barroso, E., Palomer, X., Vázquez-Carrera, M., 2020.  
830 Targeting FGF21 for the Treatment of Nonalcoholic Steatohepatitis. *Trends Pharmacol. Sci.*  
831 41, 199–208. doi:10.1016/j.tips.2019.12.005  
832

833 Zheng, Q., Martin, R.C., Shi, X., Pandit, H., Yu, Y., Liu, X., Guo, W., Tan, M., Bai, O., Meng,  
834 X., Li, Y., 2020. Lack of FGF21 promotes NASH-HCC transition via hepatocyte-TLR4-IL-  
835 17A signaling. *Theranostics* 10, 9923–9936. doi:10.7150/thno.45988  
836

837 Zhu, S., Ma, L., Wu, Y., Ye, X., Zhang, T., Zhang, Q., Rasoul, L.M., Liu, Y., Guo, M., Zhou,  
838 B., Ren, G., Li, D., 2014. FGF21 treatment ameliorates alcoholic fatty liver through  
839 activation of AMPK-SIRT1 pathway. *Acta Biochim. Biophys. Sin.* 46, 1041–1048.  
840 doi:10.1093/abbs/gmu097  
841

842 **Figure legends**



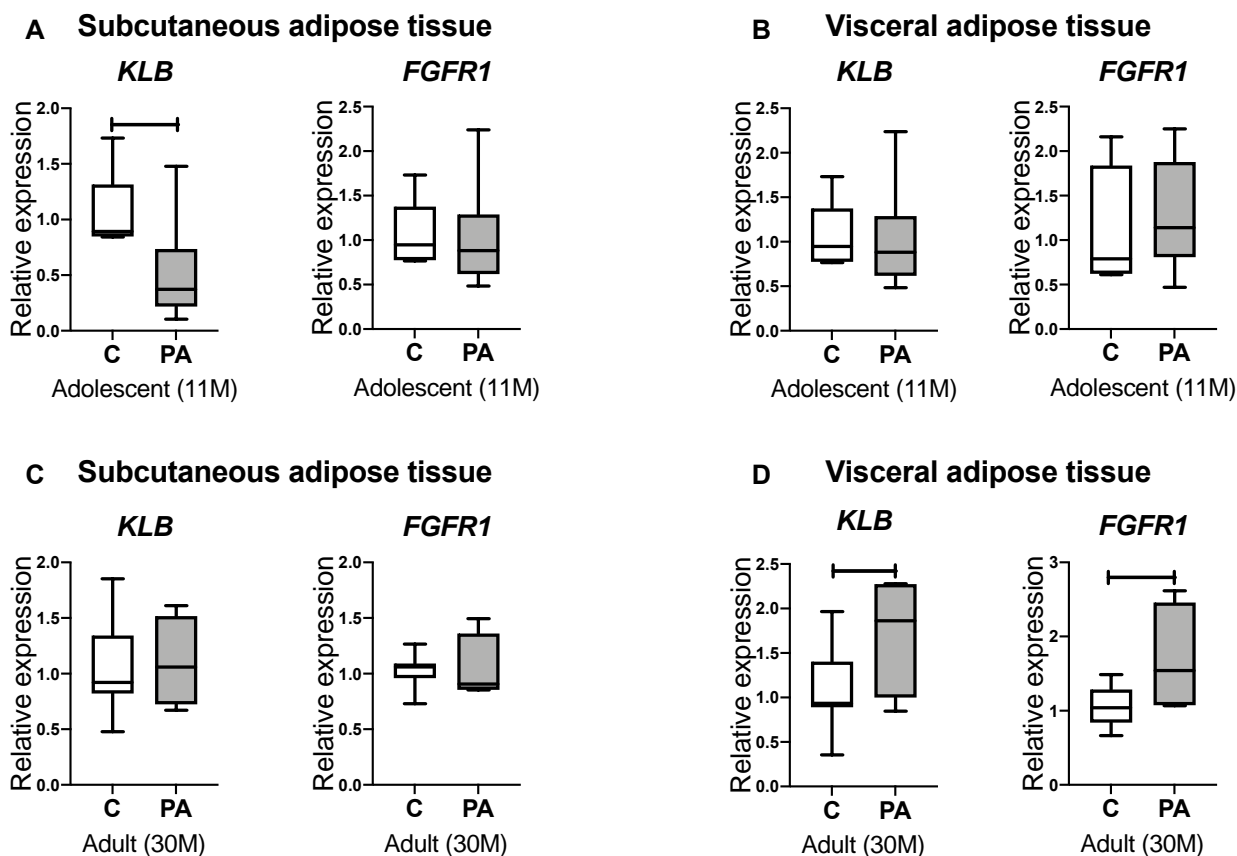
843

844 **Figure 1.** FGF21 and *PPARGC1A* expression in controls (C) and prenatally androgenised  
 845 sheep (PA) from maternal injection cohort. There was no difference in expression of *FGF21*  
 846 in (A) fetal, (B) pre-pubertal and (D) adult life. (C) Hepatic *FGF21* was reduced in  
 847 adolescent PA sheep. (E) The changes in the hepatic *FGF21* expression were mirrored by

848 circulating FGF21, with reduced levels in adolescence and in the early adulthood, that  
849 normalised in adulthood at 30 months of age. FGF21 induces PPARGC1A expression. (F)  
850 Adolescent PA sheep showed a strong trend for decreased *PPARGC1A*. (G) There was no  
851 difference in the expression of *PPARGC1A* in adulthood. (H) There was a correlation  
852 between hepatic *FGF21* and *PPARGC1A* expression in the adolescent liver. Box plot  
853 whiskers are lowest and highest observed values, box is the upper and lower quartile, with  
854 median represented by line in box. Unpaired, two-tailed Student's t test was used for  
855 comparing means of two treatment groups with equal variances accepting  $P < 0.05$  as  
856 significant. Correlation was assessed by calculation of Pearson product-moment co-  
857 efficient. (\* $P < 0.05$ ; \*\*  $P < 0.01$ ).

858





859

860

861

E

Correlation	Tissue	Animals Age	Pearson r	P value
<b><i>KLB with PPARG</i></b>	SAT	Adolescent (11M)	0.93	<0.0001
	VAT	Adolescent (11M)	0.90	<0.0001
	SAT	Adult (30M)	0.75	0.0012
	VAT	Adult (30M)	0.21	n.s.
<b><i>KLB with ADIPOQ</i></b>	SAT	Adolescent (11M)	0.80	0.0006
	VAT	Adolescent (11M)	0.65	0.013
	SAT	Adult (30M)	0.55	0.033
	VAT	Adult (30M)	0.92	<0.0001

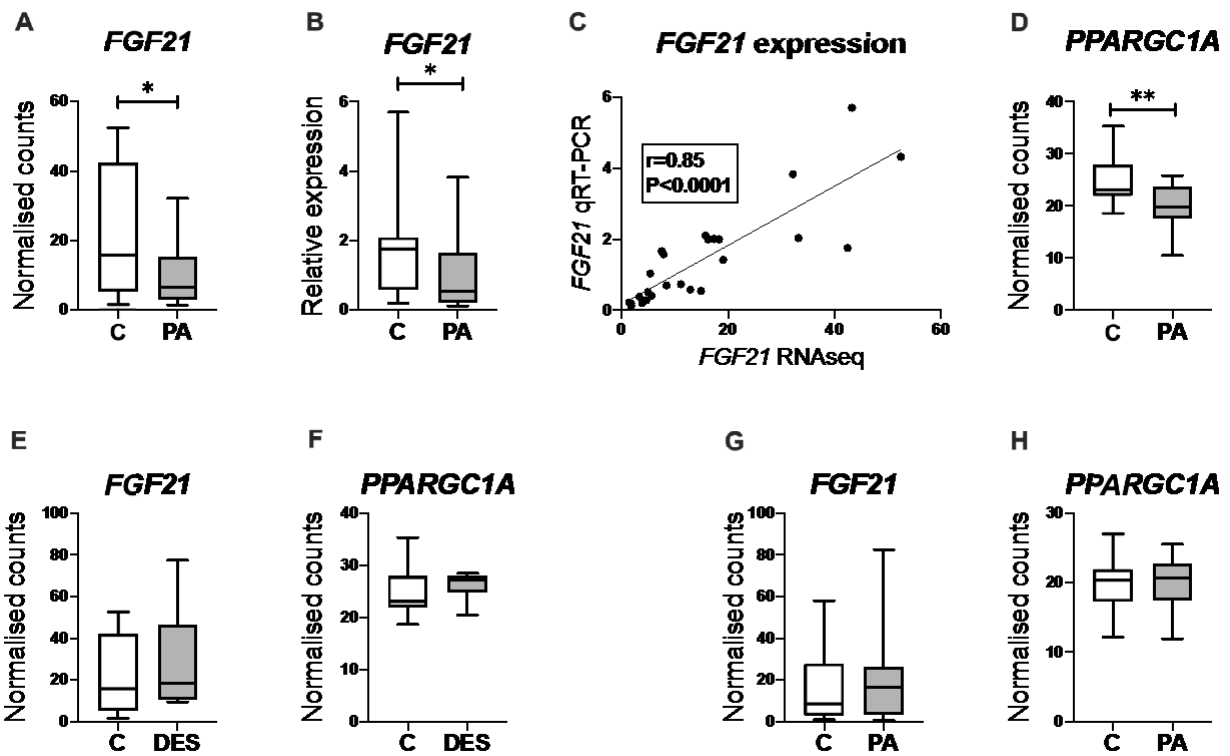
862

863 **Figure 2.** FGF21 signalling in adipose tissue in controls (C) and prenatally androgenised  
864 sheep (PA) from maternal injection cohort (androgens reached the fetuses via  
865 transplacental transfer from the mother). **(A)** In adolescence, PA sheep had reduced  
866 expression of in *KLB* in SAT, with no difference in the expression of *FGFR1*. **(B)** There was  
867 no difference in the expression of *KLB* and *FGFR1* in VAT. **(C)** In adulthood, there was no  
868 differences in *KLB* and *FGFR1* in SAT, but **(D)** both *KLB* and *FGFR1* were increased in the

869 VAT of PA sheep. (E) There was a positive correlation between *KLB* and *PPARG*  
 870 expression and *ADIPOQ* expression in both VAT and SAT, in adolescence (11 months) and  
 871 adulthood (30 months), with exception of *PPARG* in adult VAT. Box plot whiskers are  
 872 lowest and highest observed values, box is the upper and lower quartile, with median  
 873 represented by line in box. Unpaired, two-tailed Student's t test was used for comparing  
 874 means of two treatment groups with equal variances accepting  $P < 0.05$  as significant.  
 875 Correlation was assessed by calculation of Pearson product-moment co-efficient.  
 876 (\* $P < 0.05$ ).

877

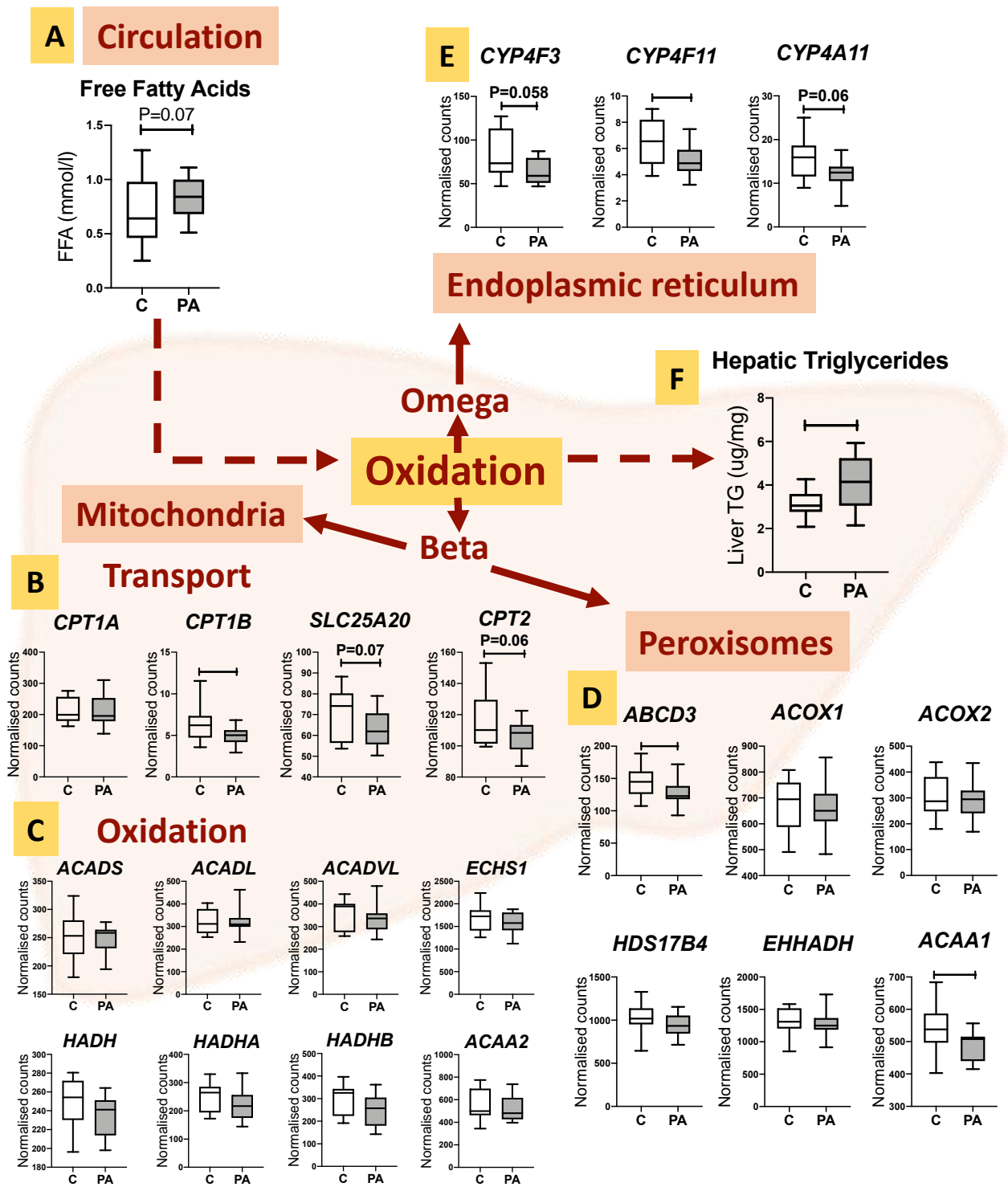
878



879

880 **Figure 3.** Hepatic *FGF21* and *PPARGC1A* expression in controls (C) and prenatally  
 881 androgenised sheep (PA) from fetal injection cohort (fetuses directly injected with androgen  
 882 during fetal life (day 62 and 82)). Adolescent female PA sheep had reduced hepatic  
 883 expression of *FGF21* when assessed through (A) RNAseq and (B) qRT-PCR, and (C) there

884 was a positive correlation between RNAseq and qRT-PCR results. (D) Adolescent PA  
885 females had decreased hepatic expression of *PPARGC1A*. (E) There was no difference in  
886 the hepatic expression of *FGF21* and (F) *PPARGC1A* in adolescent females exposed to  
887 prenatal estrogens (DES). (G) There was and no difference in *FGF21* and (H) *PPARGC1A*  
888 adolescent PA males. Box plot whiskers are lowest and highest observed values, box is the  
889 upper and lower quartile, with median represented by line in box. Unpaired, two-tailed  
890 Student's t test was used for comparing means of two treatment groups with equal  
891 variances accepting  $P < 0.05$  as significant. Correlation was assessed by calculation of  
892 Pearson product-moment co-efficient. (\* $P < 0.05$ ; \*\*  $P < 0.01$ ).

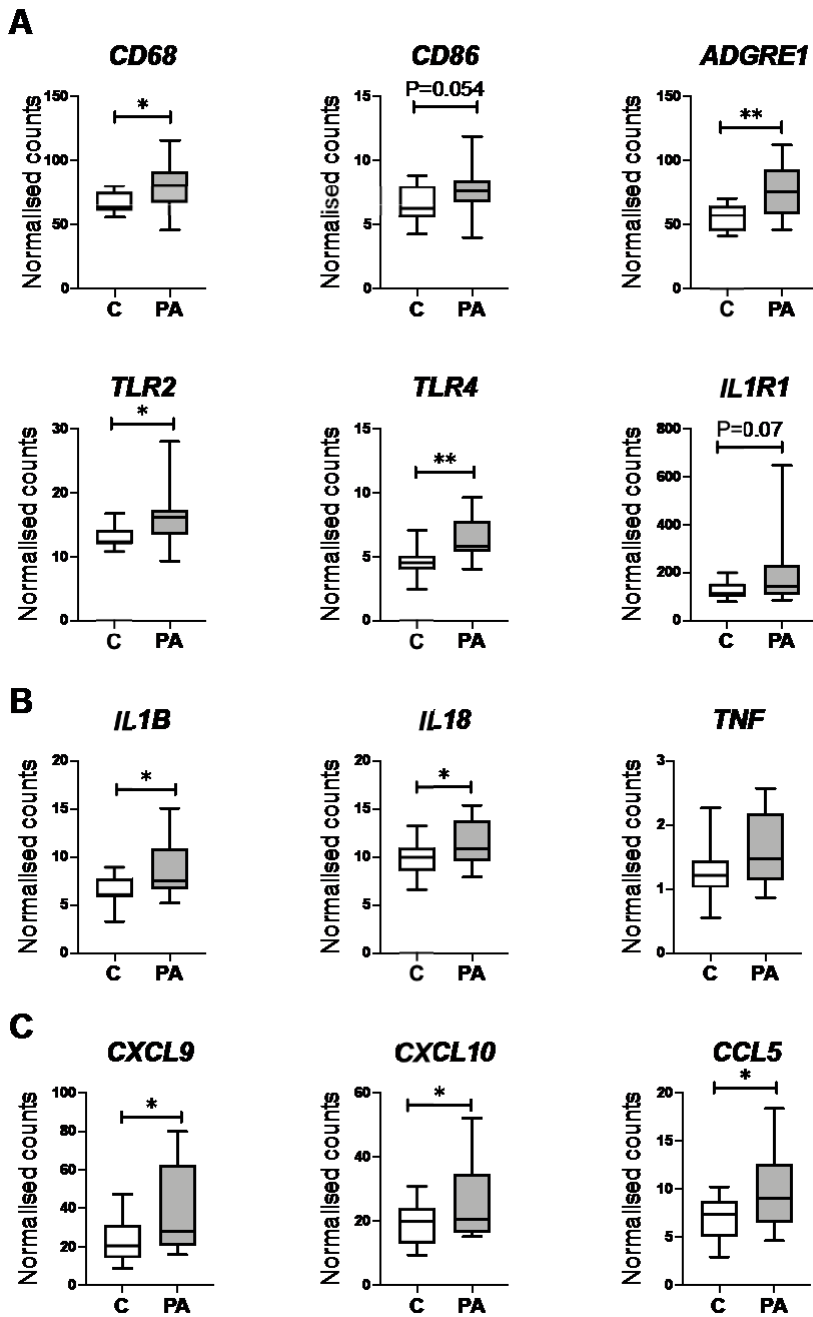


893

894

895 **Figure 4.** FFAs, hepatic oxidation and liver triglycerides in controls (C) and prenatally  
 896 androgenised sheep (PA) from fetal injection cohort. **(A)** Adolescent PA sheep had a trend  
 897 for increased circulating FFAs. **(B)** Adolescent PA sheep had decreased expression of  
 898 hepatic *CPT1B*, with a trend towards reduced expression of *SLC25A20* and *CPT2*, genes

899 involved in rate limiting mitochondrial transport of FFAs for beta oxidation. (C) There was no  
900 difference in the expression of genes associated with mitochondrial beta oxidation. (D)  
901 There was decreased expression of genes involved in the peroxisomal beta oxidation,  
902 *ABCD3* and *ACAA1*, in adolescent PA sheep. (E) Adolescent PA sheep had decreased  
903 expression of *CYP4F11* and a trend towards decreased *CYP4F3* and *CYP4A11* (Fig. 4E;  
904  $P=0.06$ ), key genes involved in omega oxidation. (F) Decreased oxidative potential in  
905 adolescent PA sheep resulted in increased hepatic triglyceride content. Box plot whiskers  
906 are lowest and highest observed values, box is the upper and lower quartile, with median  
907 represented by line in box. Unpaired, two-tailed Student's t test was used for comparing  
908 means of two treatment groups with equal variances accepting  $P<0.05$  as significant.  
909 (\* $P<0.05$ ).  
910



911

912 **Figure 5.** Molecular markers of pro-inflammatory macrophages, cytokines and chemokines

913 in liver of controls (C) and prenatally androgenised sheep (PA) from fetal injection cohort.

914 (A) Adolescent PA sheep had increased expression of molecular markers of classically

915 activated, pro-inflammatory (M1) macrophages, *CD68*, *ADGRE1*, *TLR2* and *TLR4* and a

916 trend for increased *CD86* and *IL1R1*. (B) There was increased expression of

917 proinflammatory cytokines *IL1B* and *IL18* and (C) chemokines *CXCL9*, *CXCL10* and *CCL5*

918 in PA female adolescent ewes. Box plot whiskers are lowest and highest observed values,

919 box is the upper and lower quartile, with median represented by line in box. Unpaired, two-  
920 tailed Student's t test was used for comparing means of two treatment groups with equal  
921 variances accepting  $P < 0.05$  as significant. (\* $P < 0.05$ ; \*\*  $P < 0.01$ ).

922

923 **Table 1**

Correlation with hepatic <i>PPARGC1A</i> expression		
Gene	Pearson r	P value
<i>CPT1B</i>	0.56	0.002
<i>CPT2</i>	0.49	0.011
<i>ACADL</i>	0.41	0.004
<i>HADH</i>	0.45	0.021
<i>HADHA</i>	0.40	0.042
<i>HADHB</i>	0.39	0.045
<i>ABCD3</i>	0.74	<0.0001
<i>ACOX1</i>	0.45	0.021
<i>ACOX2</i>	0.46	0.017
<i>CYP4F3</i>	0.41	0.040
<i>CYP4A11</i>	0.54	0.004

924

925 **Table 1**

926 There was a positive correlation between hepatic expression of *PPARGC1A* and genes  
927 involved in lipid oxidation in adolescent control and PA female sheep from fetal injection  
928 cohort. Correlation was assessed by calculation of Pearson product-moment co-efficient.

929

930 **Supplementary Table 1**

Gene	Forward Primer	Reverse Primer	931
<i>18S</i>	CAACTTTTCGATGGTAGTCG	CCTTCCTTGGATGTGGTA	
<i>ACTB</i>	ATCGAGGACAGGATGCAGAA	CCAATCCACACGGAGTACTTG	932
<i>FGF21</i>	TCCCGAAAGTCTCTTGGAGC	CGATCCATACAGCTTCCCATCT	933
<i>FGFR1</i>	TCAGAGACCCACCTTCAAGC	GAAGCTGGGGGAGTATTGGT	
<i>KLB</i>	CAGAGGATACCACAGCCATCT	CCAGGCTGTGTAACCAAACA	934
<i>MDH1</i>	TTATCTCCGATGGCAACTCC	GGGAGACCTTCAACAACCTTCC	935
<i>PPARGC1A</i>	ATGAGTCAGGCCACTGCAGAC	CTCTGCGGTATTCTTCCCTCT	
<i>RPS26</i>	CAAGGTAGTCAGGAATCGCTCT	TTACATGGGCTTTGGTGGAG	936

937 **Supplementary Table 1.** Primers for real-time RT-PCR analysis. Forward and reverse  
 938 primers were designed using Primer3 Input version 0.4 online software  
 939 (<http://frodo.wi.mit.edu>) with DNA sequences obtained at Ensembl Genome Browser. To  
 940 confirm the validity of the gene product in the sheep, both conventional PCR and amplicon  
 941 sequencing were performed. Primer specificity and efficacy for qRT-PCR was evaluated  
 942 through the generation of standard curves with serial dilutions of cDNA; a standard curve  
 943 slope of approximately -3.3 was accepted as efficient, and a melt-curve analysis was also  
 944 performed.

945